Journal of
Composites Science

MDPI

Article

Preliminary Experimental and Numerical Study of the Tensile Behavior of a Composite Based on Sycamore Bark Fibers

Helena Khoury Moussa [1], Philippe Lestriez [1], He Thong Bui [2], Pham The Nhan Nguyen [3], Philippe Michaud [4], Romain Lucas-Roper [4], Guy Antou [4], Viet Dung Luong [5], Pham Tuong Minh Duong [5], Fazilay Abbès [1] and Boussad Abbès [1,*]

1 MATIM, Université de Reims Champagne-Ardenne, 51100 Reims, France; helena.khoury-moussa@univ-reims.fr (H.K.M.); philippe.lestriez@univ-reims.fr (P.L.); fazilay.abbes@univ-reims.fr (F.A.)
2 University of Technology and Education, The University of Danang, Danang 55000, Vietnam; bhthong@ute.udn.vn
3 University of Science and Technology, The University of Danang, Danang 55000, Vietnam; nptnhan@dut.udn.vn
4 IRCER, University Limoges, CNRS, UMR 7315, 87000 Limoges, France; philippe.michaud@unilim.fr (P.M.); romain.lucas@unilim.fr (R.L.-R.); guy.antou@unilim.fr (G.A.)
5 Faculty of Mechanical Engineering, Thai Nguyen University of Technology, Thai Nguyen 25000, Vietnam; luongvietdung@tnut.edu.vn (V.D.L.); tuongminh80@tnut.edu.vn (P.T.M.D.)
* Correspondence: boussad.abbes@univ-reims.fr

Abstract: In the context of global sustainable development, using natural fibers as reinforcement for composites have become increasingly attractive due to their lightweight, abundant availability, renewability, and comparable specific properties to conventional fibers. This paper investigates the tensile properties of a sycamore bark fiber-reinforced composite. The tensile tests using digital image correlation showed that, by adding 18% by volume of sycamore bark for the polyester matrix, the tensile modulus achieves 4788.4 ± 940.1 MPa. Moreover, the tensile strength of the polyester resin increased by approximately 90% when reinforced with sycamore bark fiber, achieving a tensile strength of 64.5 ± 13.4 MPa. These mechanical properties are determined by the way loads are transferred between the polyester matrix and fibers and by the strength of the bond between the fiber-matrix interfaces. Since it is difficult and time consuming to characterize the mechanical properties of natural fibers, an alternative approach was proposed in this study. The method consists of the identification of the fiber elastic modulus using a finite element analysis approach, based on tensile tests conducted on the sycamore bark fiber-reinforced composites. The model correctly describes the overall composite behavior, a good agreement is found between the experimental, and the finite element predicted stress–strain curves. The identified sycamore bark fiber elastic modulus is 17,763 ± 6051 MPa. These results show that sycamore bark fibers can be used as reinforcements to produce composite materials.

Keywords: sycamore bark fiber; natural fiber; composite material; mechanical properties; finite element analysis

Citation: Khoury Moussa, H.; Lestriez, P.; Bui, H.T.; Nguyen, P.T.N.; Michaud, P.; Lucas-Roper, R.; Antou, G.; Luong, V.D.; Duong, P.T.M.; Abbès, F.; et al. Preliminary Experimental and Numerical Study of the Tensile Behavior of a Composite Based on Sycamore Bark Fibers. *J. Compos. Sci.* **2024**, *8*, 333. https://doi.org/10.3390/jcs8090333

Academic Editor: Stelios K. Georgantzinos

Received: 17 July 2024
Revised: 16 August 2024
Accepted: 21 August 2024
Published: 23 August 2024

1. Introduction

In recent decades, composite materials have garnered increasing interest due to their exceptional mechanical properties and their potential for application across various industries, including aerospace, automotive, and construction. Today, more than ever, many engineering sectors are turning to natural fiber-based composite materials due to the challenges posed by petroleum products and the need to find renewable solutions. In 2022, the global market size for natural fiber composites was valued at USD 320 million [1]. This market is projected to grow at a compound annual growth rate of 7.6% from 2023

to 2032 [1]. Natural fiber-reinforced composites present an attractive alternative to traditional composites made from synthetic fibers such as carbon, aramid, and glass across various engineering sectors [2,3]. The use of natural fibers from renewable resources offers several advantages due to their eco-friendliness, low density, low cost, and low energy consumption. Indeed, their production requires 60% less energy than the manufacturing of glass fibers [4,5] and twelve times less than that of carbon fibers [6]. However, when considering some engineering application requirements for engineering parts, such as high load-bearing performance, high strength and high modulus, and durability and fatigue resistance, synthetic fiber composites may have more advantages than natural fiber composites [7–11].

The use of natural fibers as reinforcement in composite materials is not a new concept. Numerous studies have explored the integration of fibers such as jute, sisal, flax, nettle, and bamboo, demonstrating that these fibers can enhance the mechanical properties of composites while offering significant environmental benefits [12–15].

The sycamore tree or phoenix tree (*Firmiana simplex*) [16,17] is considered a symbol of Cham Island (Vietnam). On the island, many sycamore trees are growing only on high mountain cliffs of crags. For centuries, craftsmen used sycamore bark fibers for weaving baskets, ropes, and hammocks. The tree trunk is crushed, peeled, and soaked in spring water for two to three weeks, then it is picked up and washed. The craftsmen choose the opaque white inner shell, called "manch dong". It is stripped into small fibers and dried until white to make hammocks known for their robust strength. Apart from this application, to the best of our knowledge, there are no applications of this fiber as reinforcement for composite materials. However, the literature on natural fiber-reinforced composites (NFRCs) is rich, covering different types of natural fibers that can be used as reinforcement in polymer composites, methods of production, steps involved in their processing, the mechanical properties of these composites, and their different applications [18–21]. There is a consensus on the benefits of natural fibers as potential candidates for replacing synthetic fibers as reinforcement in polymer composites because of their excellent properties such as low density, low cost, high impact resistance, high flexibility, fewer health hazards, process friendliness, low greenhouse gas emissions, and recyclability [22]. The low moisture resistance and poor wettability of natural fibers hinder their application in composites to some extent, but this can be remedied by chemical or physical treatments [23,24].

Both thermoplastic and thermoset polymers are used as matrices in natural fiber-reinforced composites. Polypropylene and polyethylene are examples of thermoplastic matrices, whereas epoxy and polyester are some of the thermosetting matrices commonly used [18]. The reinforcement of polyesters with cellulosic fibers has been widely reported, including polyester–jute [25,26], polyester–sisal [27], polyester–coconut [28], and polyester–straw [29]. They are widely produced industrially as they have many advantages compared to other thermosetting resins including room temperature cure capability, good mechanical properties, and transparency.

A study investigated the moldability and interfacial adhesion strength of polypropylene composites using wood by-products from roadside tree pruning, with a specific emphasis on American sycamore (*Platanus occidentalis* L.) [30]. While research has extensively explored the utilization of sycamore leaves for value-added products like particleboard, highlighting their promising mechanical properties and potential in furniture manufacturing [31,32], there remains a notable gap in the literature regarding the use of sycamore fibers. To the best of our knowledge, there is no scientific publication related to the mechanical properties of the sycamore bark fibers and their composites.

This study seeks to fill this gap by focusing on the experimental characterization and numerical modeling of composite materials reinforced with sycamore bark fibers, aiming to explore their potential as a sustainable alternative to traditional synthetic fibers.

2. Materials and Methods

2.1. Materials

Two main materials were used in this study: polyester resin and sycamore bark fiber. The polyester resin, supplied by SOLOPLAST-VOSSCHEMIE (Fontanil-Cornillon, France), was used as the matrix for the composite material and has a density of 1.1 g/cm^3 and a viscosity 0.55 Pa·s at 20 °C. The sycamore bark fibers, sourced from Vietnam, served as the reinforcement. These interlocking fibers, which naturally have a unique tissue-like structure, as shown in Figure 1, were used in their original form for this study.

Figure 1. Sycamore bark fiber tissue-like structure.

2.2. Fiber's Extraction

The production of sycamore fiber begins with the careful harvesting of young trees, typically found in remote, high-altitude locations or on steep cliffs. These trees, about one arm's length long, are selectively cut and bundled before being transported down from the mountains to lower elevations. Once brought to accessible areas, the tree trunks undergo a meticulous process. They are immersed in streams, where they soak for extended periods—up to half a month in summer and over 20 days in winter. Following this soaking period, the bark is methodically cleaned, peeled, and pounded on stones to soften and separate the fibers [33]. The main steps concerning this extraction process are outlined and illustrated in Figure 2. These fibers are originally used for knitting sycamore hammock, a typical handicraft of the Cham Island people for a long time. The process used is still artisanal. For use in industrial applications, the entire process would have to be improved and automated to make it more efficient.

Figure 2. Extraction process of sycamore bark fibers, from the plant to the fibers.

2.3. Fabrication of Sycamore Bark Fiber-Reinforced Composite

The sycamore bark fiber-reinforced composite was produced using the conventional hand layup process on a glass plate, followed by compression with another glass plate, as shown in Figure 3. Before manufacturing, the sycamore fibers were conditioned at 23 ± 1 °C and 50 ± 1% relative humidity for 7 days.

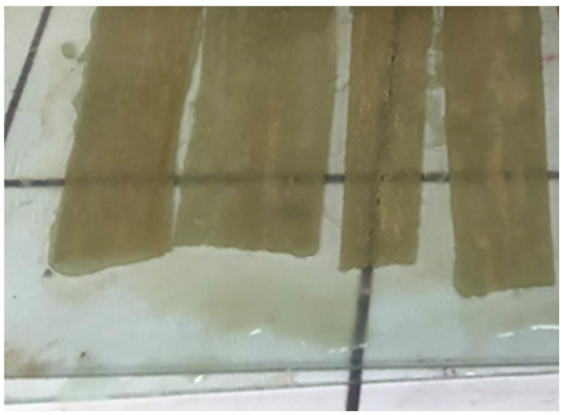

Figure 3. Sycamore bark fiber-reinforced composite plate before cutting.

A release wax supplied by SOLOPLAST-VOSSCHEMIE (Fontanil-Cornillon, France) was applied to the mold as a thin film. The polyester resin, prepared following the rule of weighing the fibers and multiplying by 2.5 to determine the required resin weight, was carefully mixed with a 2% weight of methyl ethyl ketone peroxide (MEKP) hardener according to the supplier's instructions. A first layer of resin was spread on the glass plate. The sycamore fibers were then placed on this layer, and a second layer of resin was applied over the fibers using a paintbrush to embed them thoroughly. Immediately following this, an aluminum bubble paddle roller was used to remove any trapped air bubbles.

Once the impregnation was completed, an upper glass plate was placed over the setup and compressed using weights. The prepared composite was left to cure in the mold at ambient temperature. After 24 h, the curing process was complete, and the composites were removed from the glass plates and were cut for mechanical testing. The volume fraction of the fibers used in this study was $V_f = 18\%$.

In this study, the conventional hand layup process was used to prepare the composite samples, and manual fiber positioning and impregnation is not optimal, as can be seen in Figure 3. To prepare products of regular shape and size when considering engineering applications, the fiber strips can be aligned and joined together to form a continuous web. A vacuum infusion process can also be used to improve resin distribution.

2.4. Tensile Tests

Eight tensile tests were conducted on the composite material in accordance with ISO 527-5 standard [34]. Additionally, five tensile tests were performed on pure polyester specimens in the form of standard dumbbell-shaped test specimens following ISO 527-2 [35].

Specimens were tested on a tensile machine (MTS Criterion Model 43, Créteil, FRANCE) equipped with a 5 kN loading cell. The specimens were loaded to failure at a strain rate of 2 mm/min and room temperature. Local displacements and strains within the effective region were measured using a Digital Image Correlation (DIC) setup. This DIC system consists of two high-resolution cameras equipped with 35 mm focal length lenses and DIC post-processing software v6.1 (Aramis, Germany) [36]. The DIC method has demonstrated reliable results comparable to strain gauge measurements [37,38]. Before testing, the specimens were prepared by painting them with white color acrylic resin-based paint for contrast, followed by spraying with black color acrylic resin-based paint, creating stochastic black and white contrast patterns on the surface, as illustrated in Figure 4.

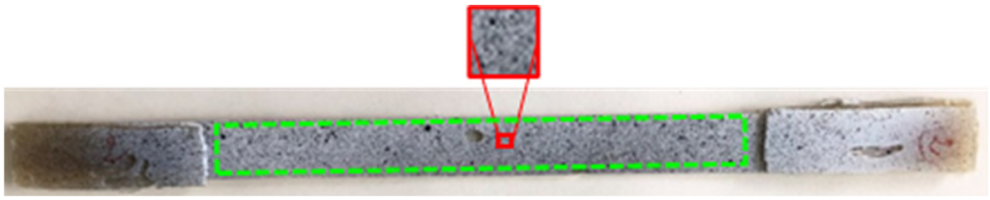

Figure 4. Composite sample coated with stochastic black and white contrast patterns.

After preparing the specimen with the appropriate pattern and setting up the measurement apparatus and loading device, images were acquired during deformation with a frequency of 1 Hz. To perform DIC, an area of interest is specified as shown in Figure 4 (dashed green line). The area is divided into an evenly spaced virtual grid of 20 × 20 pixels (red square subset in Figure 4). The displacements are computed at each point of the virtual grids to obtain full-field deformation by comparing the reference image (before deformation) to deformed images.

2.5. Microstructural Observations

The fiber surface morphology was examined using a Quanta FEG 450 SEM (FEI, Hillsboro, Oregon, USA). The SEM operated at an acceleration voltage of 1 kV and a working distance of approximately 15 mm. The acquired images were processed with the ImageJ software v1.54 [39] to measure the cross-section area of each fiber. An interactive contour line was drawn to outline the fiber cross section (Figure 5), after which the area was measured, and the equivalent diameter was calculated.

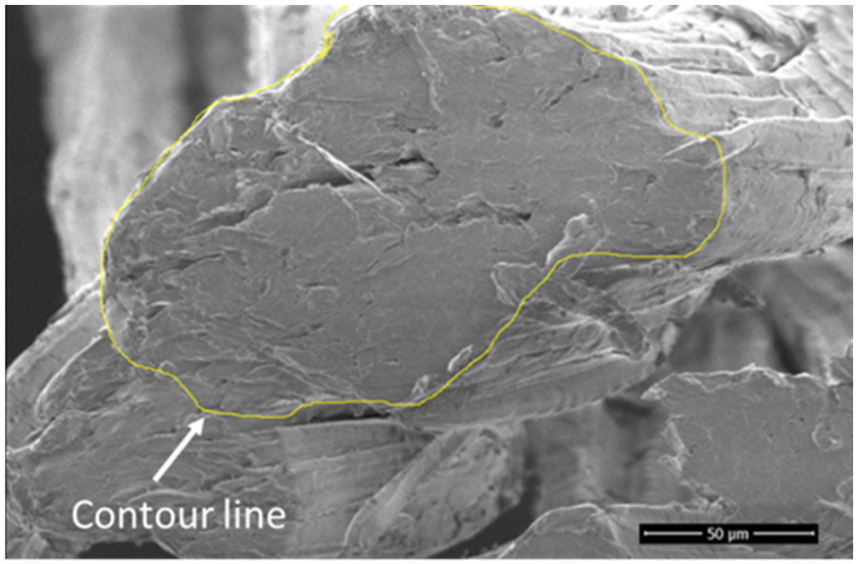

Figure 5. Cross-section area measurement using ImageJ.

3. Finite Element Modeling

3.1. Modeling Hypotheses

Since it is experimentally difficult to carry out tensile tests on the tissue-like structure of the sycamore bark fiber (Figure 1) to determine its mechanical properties, we propose to use finite element numerical simulation to estimate them. A similar approach was used by Abida et al. [40] for the identification of flax yarns' mechanical properties.

An example of the geometry model of the composite test specimen is shown in Figure 6, where the tissue-like structure of the sycamore bark fiber was reconstructed from an image and embedded in a resin matrix.

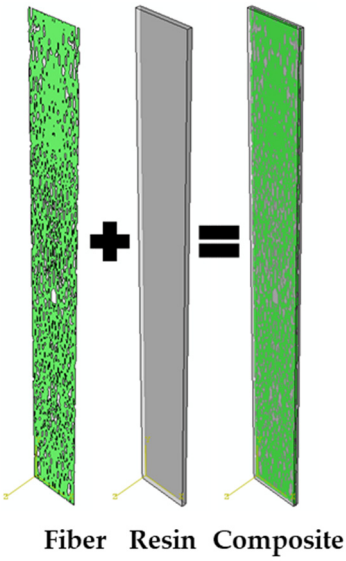

Figure 6. Geometry model of the composite test specimen.

The aim of our modeling is to use an inverse approach to determine the elastic modulus of the sycamore bark fibers. Furthermore, the stress–strain curves given in the next section show linear brittle behavior. For this purpose, the mechanical behaviors of the resin, the fiber, and the composite were considered to be linear elastic. As a first approach, a perfect bonding between the fibers and the matrix is assumed. Advanced approaches, such as cohesive zone modeling (CZM) [41,42], can be used in future work to model the fiber–matrix interface. The elastic modulus and Poisson ratio of the resin are experimentally determined from the tensile tests and used in the simulations. The elastic modulus and Poisson ratio of the fibers are iteratively tuned until the experimental tensile curve of the composite is superimposed with the numerical one.

3.2. Simulation Setup

The numerical model was developed to conduct a static study using the finite element software ABAQUS 2019 [43]. To simulate the tensile test of the composite sample, rigid plates were tied to both ends of the test sample to represent the tensile jaws. The simulation setup involves applying a displacement in the y direction (U_y) to the top rigid plate, while the bottom plate was fully constrained, as shown in Figure 7.

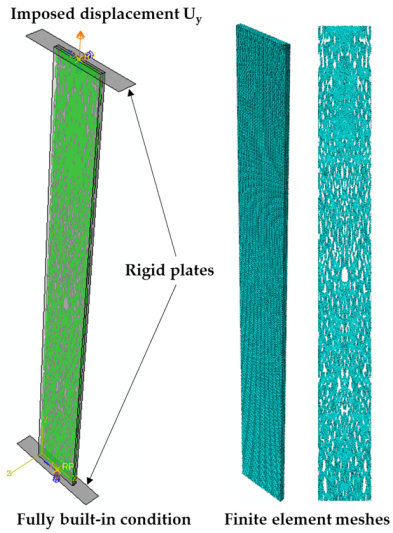

Figure 7. Boundary conditions and finite element meshes.

The resin was modeled as a 3D part and meshed using 3D, eight-node, linear, brick (C3D8R) elements with reduced integration and hourglass control. The tissue-like fiber structure was modeled as a 3D shell part and meshed using three-node triangular general-purpose shell and finite membrane strain (S3) elements. A mesh size of 0.25 mm was set, leading to 163,200 brick elements for the resin and 132,421 shell elements for the fiber (Figure 7).

A mesh sensitivity analysis was conducted on the composite sample to see how the simulation results vary with mesh element size. The analysis was conducted by changing the element size with a mesh size control of 2 mm, 1 mm, 0.5 mm, 0.25 mm, and 0.15 mm, giving the following element numbers: 38,056, 63,640, 105,541, 295,621, and 1,071,554, respectively. The maximum stress obtained was then plotted against the number of elements in Figure 8, indicating that, for a mesh size lower than 0.25 mm, the maximum stress varies very little with the subsequent mesh.

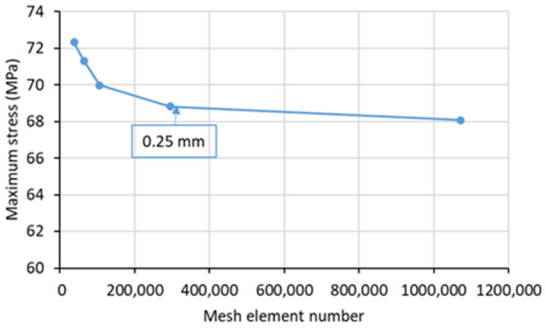

Figure 8. Mesh sensitivity analysis.

4. Results and Discussion

4.1. Experimental Results of Tensile Tests

The tensile stress versus strain curves for the resin and the composite are shown in Figure 9. It can be seen that the curves have many fluctuation points. These fluctuations are due to the noise-induced bias that affects DIC strain field measurements [44,45]. Different filtering options can be used to reduce the noise; however, the filtering of these fields influences measured strain gradients [46,47]. Analyzing these preliminary data, it is noticed that, as expected, the tensile curves of the polyester resin and the sycamore bark fiber-based composite show a quasi-elastic brittle behavior. It is also clear from the plots that the tensile load-bearing capacity has improved for fiber-reinforced composite; polyester resin samples failed at low stress amongst the composites.

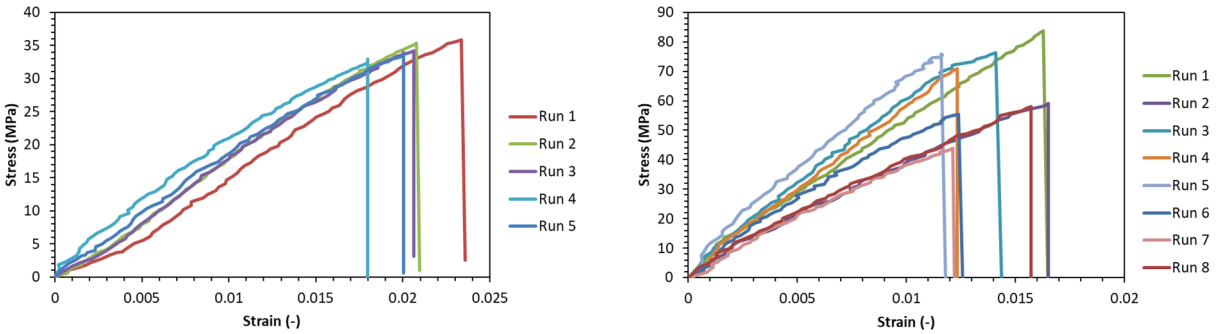

(**a**) Resin stress–strain curves (**b**) Composite stress–strain curves

Figure 9. Experimental stress–strain curves.

Figure 10 illustrates five color maps of the longitudinal strain field of the composite material at various stages of deformation up to the point of failure and the corresponding

points on the tensile stress–strain curve. The color maps indicate a relatively uniform strain distribution across the specimen. This suggests that the material responds homogeneously to the applied tensile load, indicating a good load distribution and efficient stress transfer among the composite components. As deformation progresses, higher strain values become localized in the middle of the gage region, suggesting the onset of localized deformation.

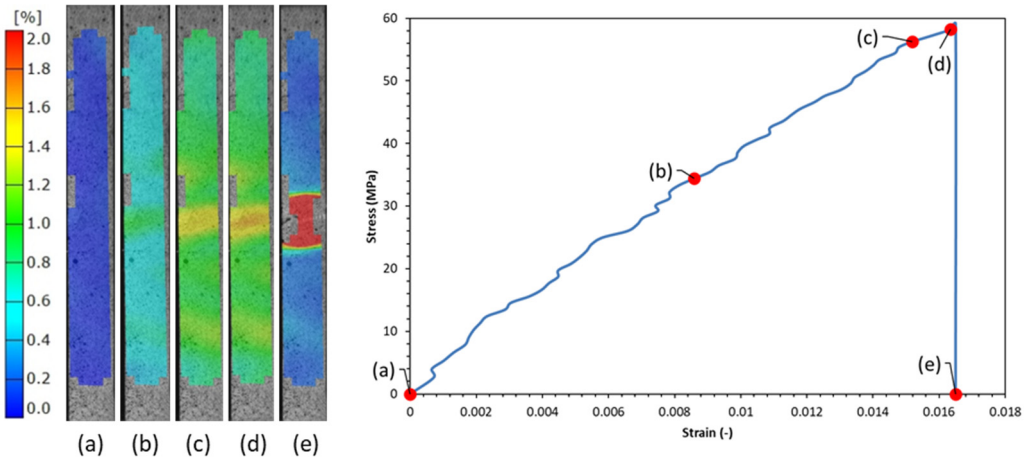

Figure 10. Strain distribution at five different loading stages and corresponding stress vs. strain curve for composite.

Reinforcing a polymer matrix with sycamore fibers significantly enhances its mechanical properties. The results of all tensile tests performed on both the pure resin and composite samples are listed in Table 1. Figure 11 illustrates the comparison of the mechanical properties between the resin and the composite, highlighting the improvements achieved through the inclusion of sycamore fibers. As shown in Figure 11a, the elastic modulus of the polyester matrix, originally 1916 MPa, increased by about 150% with the inclusion of sycamore fiber. Additionally, the tensile strength of the polyester resin increased by approximately 90% when reinforced with sycamore bark fibers, achieving a tensile strength of 64.5 MPa (see Figure 11c).

Table 1. Mechanical properties of resin and composite.

Samples	Resin				Composite			
	Modulus (MPa)	Poisson Ratio (-)	Max. Stress (MPa)	Max. Strain (-)	Modulus (MPa)	Poisson Ratio (-)	Max. Stress (MPa)	Max. Strain (-)
1	1848.3	0.42	35.9	2.33%	4878.4	0.31	83.8	1.63%
2	1973.1	0.39	35.4	2.08%	4013.6	0.29	59.2	1.65%
3	1988.4	0.40	34.2	2.06%	5690.7	0.34	76.3	1.41%
4	1949.8	0.41	33.0	1.80%	5652.4	0.39	70.8	1.23%
5	1823.4	0.39	33.9	2.01%	6124.2	0.45	76.0	1.16%
6					4363.0	0.43	55.4	1.24%
7					3608.2	0.45	43.9	1.21%
8					3976.4	0.41	58.1	1.57%
Mean	1916.6	0.40	34.5	2.06%	4788.4	0.38	65.4	1.39%
Std. Dev.	75.5	0.01	1.2	0.19%	940.1	0.06	13.4	0.19%

These findings align with several studies focused on natural fiber-reinforced polyester composites [48]. For instance, research on hybrid composites of natural fiber and glass fiber in a polyester matrix demonstrated similar enhancements. Muthukumar et al. [49] showed that the tensile load-carrying capacity of the jute/glass composite, approximately 35 MPa, is 1.94 and 1.59 times higher than those of sisal/glass and kenaf/glass composites,

respectively. Abbès et al. [13] found that the modulus of polyester resin increased by 101% with the addition of 12% by weight glass and 6% by weight nettle fibers. Additionally, the mechanical properties of sisal- and hemp-reinforced polyester resin composites were found to increase with higher fiber weight fractions [50]. The improvement in tensile strength was 110% for hemp and 94.45% for sisal fiber. The strength further increased when hemp and sisal fibers were combined.

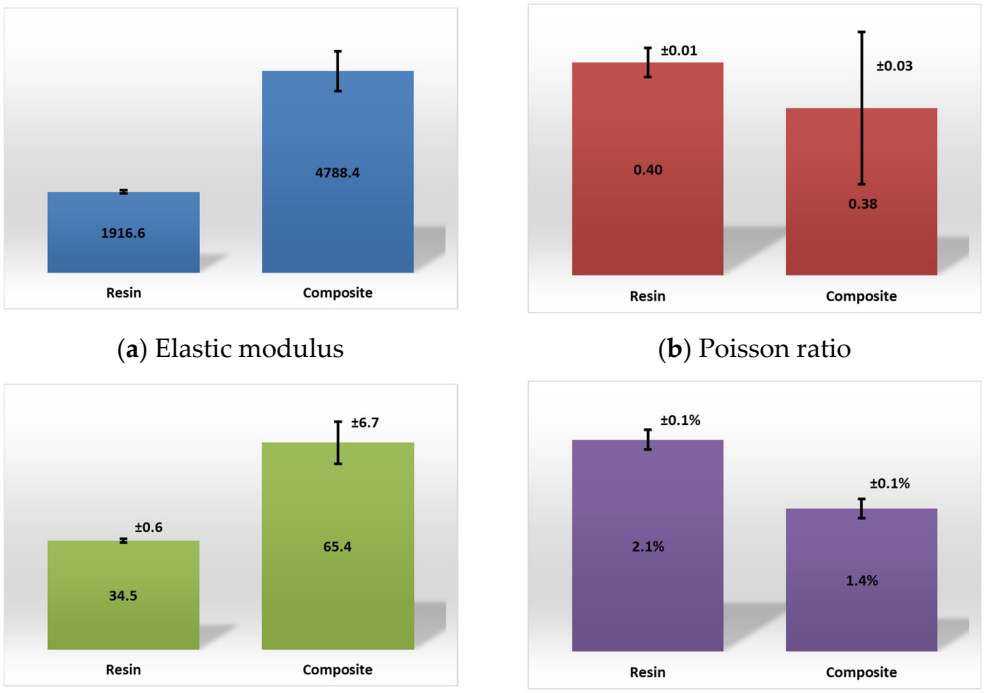

(**a**) Elastic modulus (**b**) Poisson ratio

(**c**) Maximum stress (**d**) Maximum strain

Figure 11. Comparison of mechanical properties of resin and composite.

The results indicate that sycamore fibers are a viable reinforcement material, providing comparable mechanical enhancements relative to other natural fibers. This improvement in mechanical properties highlights the potential of sycamore fiber composites in various applications requiring enhanced tensile strength and modulus.

These first results show that the strength of the polyester resin–sycamore bark fiber composite is higher than that of composites with fiberglass at similar fiber volume fraction [51]. However, the adhesion of sycamore bark fiber with polyester resin was not investigated and may be lower than that of fiberglass. This can affect the long-term durability performance of the composite, despite its initial high strength characteristics. The long-term durability performance and degradation behavior under various aging environments (thermo-oxidative aging, accelerated weathering (ultraviolet aging), hydrolytic degradation, fatigue, and creep, etc.) of natural fiber-reinforced composites are very important and need to be explored. Chang et al. [52] reviewed studies on the durability of biobased composites and discussed future perspectives and methods to improve the durability performance of these materials. Various physical and chemical processes to enhance the durability and strength of natural fiber exist, including plastination technique [53], plasma treatment [54], electron radiation [55], and chemical treatments [56–58].

According to Figure 11b, the experimental Poisson's ratio for the sycamore bark fiber composite exhibited significant variability, with a standard deviation of 0.06 across eight different tests. The natural and specific structure of sycamore bark fibers, characterized by interlocking fibers, likely contributes to this variability. Differences in fiber properties, distribution, and orientation within the composite can lead to varying Poisson's ratios in different samples.

There is a perceived problem with plant fibers related to the variability of the properties of these natural materials [59]. Some factors affect variability, from plant growth conditions to fiber selection and testing. This variability occurs at several scales, including composition, morphology, surface finish, and mechanical properties, all of which define the overall quality, which can differ between crops [60]. However, Bayley et al. [60] showed that by carefully controlling the fiber supply, using appropriate characterization procedures, and optimizing manufacturing processes, excellent composite properties can be achieved with low variability.

Regarding the strain at break, it decreased from 2.1% to 1.4% after the addition of sycamore bark fibers to the polyester matrix. This reduction indicates that while the composite material becomes stronger and more rigid due to the fiber reinforcement, it also becomes less ductile. The fibers restrict the matrix's ability to deform, leading to a lower strain at break. This trade-off between increased strength and reduced ductility is common in fiber-reinforced composites. We should also note that the measured strain at break exhibited a considerably low standard deviation among the eight tested composite specimens. This consistency suggests that the fiber structure did not significantly influence the rupture behavior of the composite.

4.2. Microstructural Analysis

The surface morphology of the sycamore fibers was examined using scanning electron microscopy at different magnifications and it is shown in Figure 12a–d. It was important to study the surface morphology of the fibers to determine their ability to act as a good reinforcement and to resist fiber pull out. Figure 12a,b show the surface morphology of a bundle of sycamore fibers. It consists of several elementary fibers like fibrils bonded together with the direction of their length of fibers to form a bundle. Moreover, fiber cells are almost cylindrical in shape and compactly arranged. Figure 12b shows that the transverse section of the structural fibers is found in semi elongated circular shapes. Figure 12c,d reveal the presence of shallow pores and a regular non-smooth surface structure which increases the surface roughness of the fiber. The surface roughness of the fiber provides better bond strength of the fiber to the matrix in the manufacturing of polymer composites [61–63].

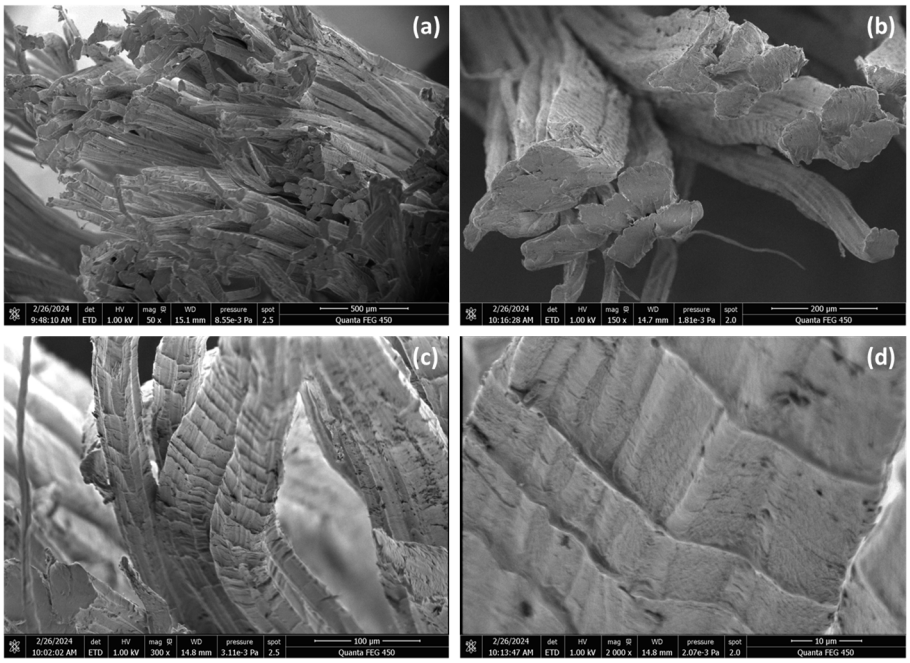

Figure 12. SEM micrographs of the sycamore bark fibers bundle at different magnifications: (**a**) 50×, (**b**) 150×, (**c**) 300× and (**d**) 2000×.

The diameter distribution of the bundles is depicted in Figure 13, showing a normal distribution with a mean diameter of 84.9 µm and a standard deviation of 18.8 µm.

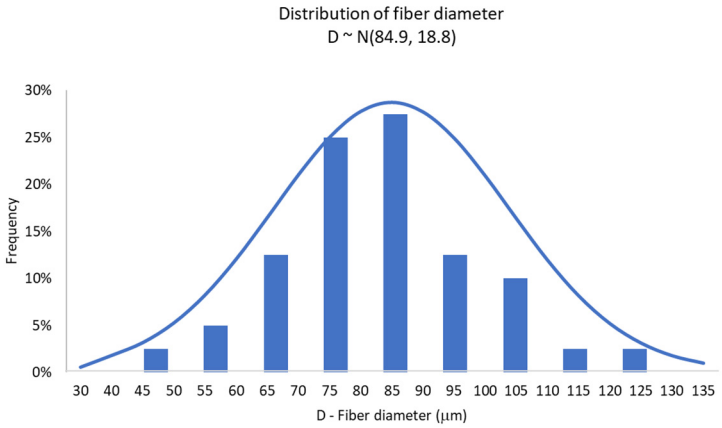

Figure 13. Diameter distribution of sycamore bark fiber bundles.

4.3. Finite Element Simulation Results

To determine the fiber elastic modulus from experimental tensile tests on composite specimens, eight finite element simulations were run, as defined in Section 3, corresponding to the eight tested composite specimens. The elastic modulus of the fiber was tuned to minimize the difference between the measured and the computed composite tensile curve. As can be seen in Figure 14, the model correctly describes the overall composite behavior. A good agreement is found between the experimental and the finite element predicted stress–strain curves. However, some discrepancies are observed between numerical and experimental results. This can be attributed to the following different hypotheses in the modeling: the composite failure was not considered in this study and a linear elastic behavior is assumed; for each sample, the thickness is assumed to be constant in the tissue-like structure; and the model uses a continuous shell element, which does not take into account the discontinuous aspect of the fibers.

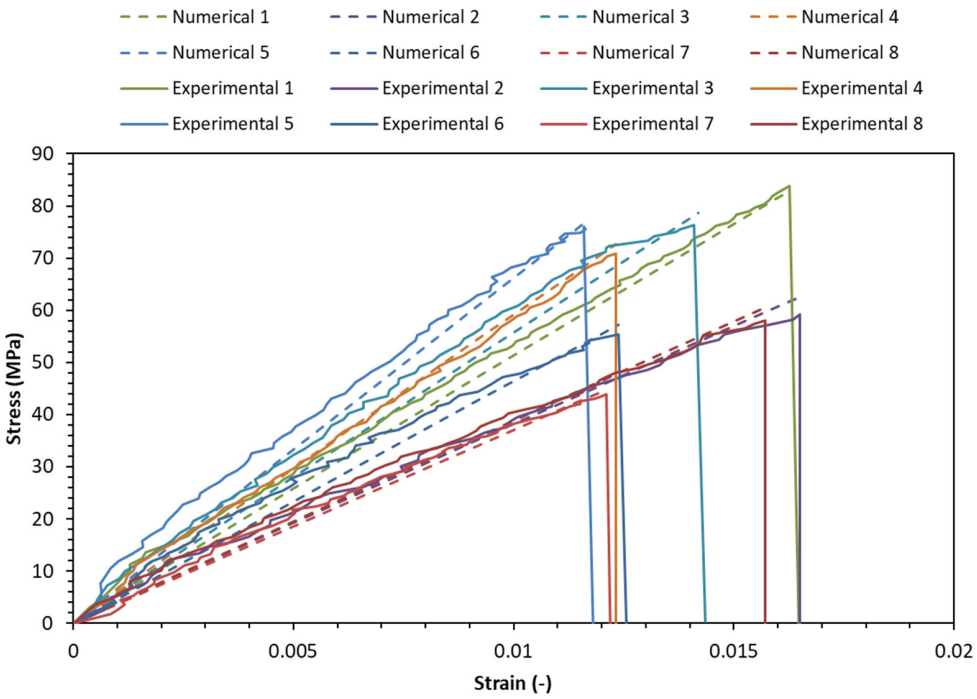

Figure 14. Comparison between experimental and predicted composite behavior.

The identified sycamore bark fiber moduli are summarized in Table 2. Finite element simulations were run on the fibers and the obtained numerical tensile curves are plotted in Figure 15, showing a large dispersion induced by the dispersion in the identified moduli (17,763 ± 6051 MPa). Abida et al. [40] and Belaadi et al. [64] pointed out the same conclusions in studies on sisal and flax fibers, respectively. De Andrade Silva et al. [65] also found that the elastic modulus of sisal fibers varies between 9000 and 19,000 MPa. Kim and Netravali [66] found an elastic modulus of 11,910 MPa for aligned-hemp yarns, and Blanchard et al. [67] measured an elastic modulus of 11,400 ± 2110 MPa for flax yarns.

Table 2. Identified modulus for sycamore bark fiber.

Samples	Modulus (MPa)
1	19,500
2	11,200
3	22,400
4	22,600
5	27,200
6	15,600
7	11,300
8	12,300
Mean	17,763
Std. Dev.	6051

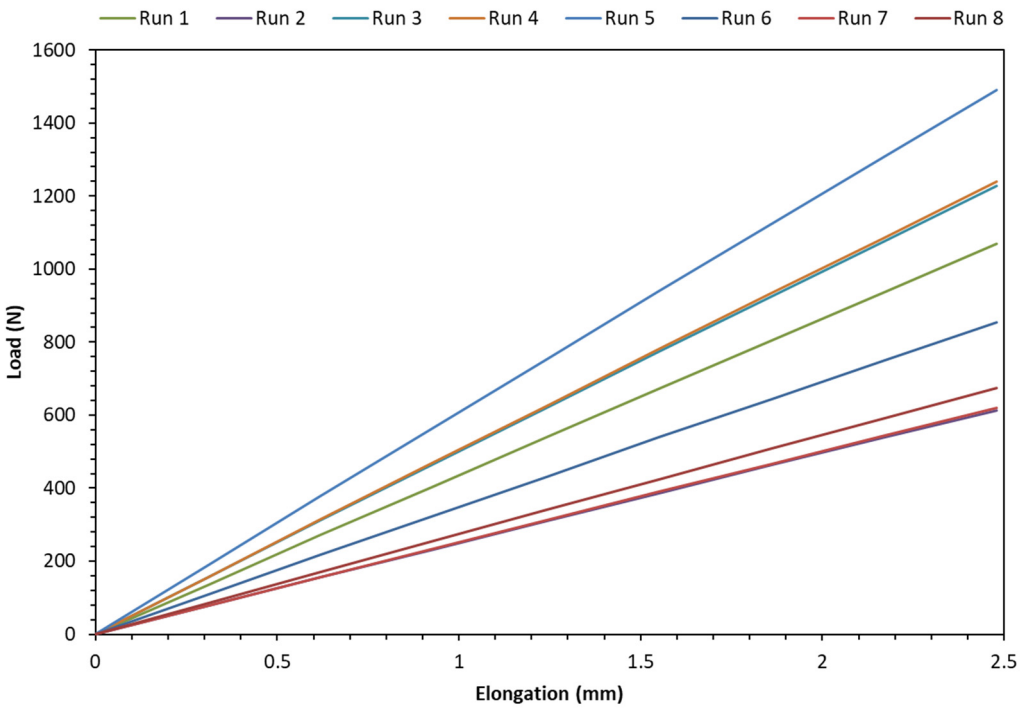

Figure 15. Numerical tensile curves of sycamore bark fibers.

5. Conclusions

The purpose of this study was to characterize the tensile behavior of sycamore bark fiber-reinforced composite and to develop a numerical strategy to determine the elastic modulus of these fibers from tests performed on the composite. The main conclusions obtained in this study are the following:

- The experimental tensile tests using DIC strain field measurements show that the addition of sycamore bark fibers to the polyester matrix significantly incremented the elastic modulus from 1916.1 to 4788.4 MPa up to 18 vol.% of reinforcement, corresponding to an increment of 150%.

- Additionally, the tensile strength of the polyester resin increased by approximately 90% when reinforced with sycamore bark fibers, attaining a tensile strength of 64.5 MPa.
- The strain at break decreased from 2.1% to 1.4% after the addition of sycamore bark fibers to the polyester matrix. This reduction indicates that the composite material becomes stronger and more rigid due to the fiber reinforcement; it also becomes less ductile.
- The microstructural analysis revealed that the fiber cells are almost cylindrical in shape and compactly arranged, and the transverse section of the structural fibers is found in a semi elongated circular shape. The diameter distribution of the bundles shows a normal distribution with a mean diameter of 84.9 µm and a standard deviation of 18.8 µm.
- From experimental tensile tests on composite specimens, an inverse problem was solved to evaluate the elastic modulus of the fibers. The models delivered an average elastic modulus of 17,763 $\pm$ 6051 MPa, which were found in the same order of magnitude as other existing natural fibers despite the observed variability inherent to the natural fibers.

This paper demonstrated the potential of using sycamore bark fibers to enhance the properties of polyester matrices for various applications; however, further research is required:

- Prior to industrial applications, supplementary research should be performed to assess the materials' long-term durability performance and degradation behavior under various aging environments (thermo-oxidative aging, accelerated weathering (ultraviolet aging), hydrolytic degradation, fatigue, and creep, etc.).
- The potential of sycamore bark fiber should be analyzed considering its mechanical performance along with its sustainability aspects. For this assessment, life cycle assessment (LCA) can be deployed to evaluate the environmental aspects and potential impacts of the entire product's life cycle.
- Advanced approaches, such as cohesive zone modeling (CZM), can be investigated in future work to model the fiber-matrix interface.

Author Contributions: Conceptualization, P.L., H.T.B. and B.A.; Data curation, B.A.; Investigation, H.K.M., P.M., R.L.-R., G.A. and V.D.L.; Methodology, H.K.M., V.D.L. and P.T.M.D.; Resources, P.L., H.T.B. and B.A.; Software, P.L. and F.A.; Supervision, P.L., H.T.B. and B.A.; Validation, P.T.N.N., P.M. and P.T.M.D.; Writing—original draft, H.K.M. and B.A.; Writing—review and editing, H.K.M., H.T.B., P.T.N.N., R.L.-R., G.A., F.A. and B.A. All authors have read and agreed to the published version of the manuscript.

Funding: This research received no external funding.

Data Availability Statement: All data used to support the findings of this study are included within the article.

Conflicts of Interest: The authors declare no conflicts of interest.

References

1. Natural Fiber Composites Market—By Type (Wood Fiber Composites, Hemp Fiber Composites, Flax Fiber Composites, Jute Fiber Composites), by Matrix (Inorganic Compound, Natural Polymer, Synthetic Polymer), by End-Use & Forecast, 2023–2032. Global Market Insights Inc. Available online: https://www.gminsights.com/industry-analysis/natural-fiber-composites-market (accessed on 6 June 2024).
2. Thakur, V.K.; Thakur, M.K.; Gupta, R.K. Synthesis of lignocellulosic polymer with improved chemical resistance through free radical polymerization. *Int. J. Biol. Macromol.* **2013**, *61*, 121–126. [CrossRef]
3. Saha, P.; Chowdhury, S.; Roy, D.; Adhikari, B.; Kim, J.K.; Thomas, S. A brief review on the chemical modifications of lignocellulosic fibers for durable engineering composites. *Polym. Bull.* **2016**, *73*, 587–620. [CrossRef]
4. Azwa, Z.N.; Yousif, B.F.; Manalo, A.C.; Karunasena, W. A review on the degradability of polymeric composites based on natural fibres. *Mater. Des.* **2013**, *47*, 424–442. [CrossRef]
5. Brosius, D. Natural fiber composites slowly take root. *Compos. Technol.* **2006**, *12*, 32–37.

6. Dujardin, N. Un matériau biosourcé de choix: Les fibres naturelles. Caractérisations et applications. In *25èmes Journées Scientifiques de l'Environnement-L'économie Verte en Question* (No. 01). 2014. Available online: https://hal.science/hal-00978360 (accessed on 4 June 2024).
7. Correia, J.R.; Cabral-Fonseca, S.; Branco, F.A.; Ferreira, J.G.; Eusébio, M.I.; Rodrigues, M.P. Durability of pultruded glass-fiber-reinforced polyester profiles for structural applications. *Mech. Compos. Mater.* **2006**, *42*, 325–338. [CrossRef]
8. Panaitescu, I.; Koch, T.; Archodoulaki, V.M. Accelerated aging of a glass fiber/polyurethane composite for automotive applications. *Polym. Test.* **2019**, *74*, 245–256. [CrossRef]
9. Dong, Z.; Ji, J.H.; Liu, Z.Q.; Wu, C.; Wu, G.; Zhu, H.; Zhang, P. I-shaped ECC/UHPC composite beams reinforced with steel bars and BFRP sheets. *Sustain. Struct.* **2023**, *3*, 000022. [CrossRef]
10. Ke, L.; Li, Y.; Li, C.; Cheng, Z.; Ma, K.; Zeng, J. Bond behavior of CFRP-strengthened steel structures and its environmental influence factors: A critical review. *Sustain. Struct.* **2024**, *4*, 000038. [CrossRef]
11. Xian, G.; Zhou, P.; Bai, Y.; Wang, J.; Li, C.; Dong, S.; Guo, R.; Li, J.; Du, H.; Zhong, J. Design, preparation and mechanical properties of novel glass fiber reinforced polypropylene bending bars. *Constr. Build. Mater.* **2024**, *429*, 136455. [CrossRef]
12. Alam, L.; Piezel, B.; Sicot, O.; Aivazzadeh, S.; Moscardelli, S.; Van-Schoors, L. UV accelerated aging of unidirectional flax composites: Comparative study between recycled and virgin polypropylene matrix. *Polym. Degrad. Stab.* **2023**, *208*, 110268. [CrossRef]
13. Abbès, F.; Xu, S.; Abbès, B. Characterization of Mechanical and Damping Properties of Nettle and Glass Fiber Reinforced Hybrid Composites. *J. Compos. Sci.* **2022**, *6*, 238. [CrossRef]
14. Chauhan, V.; Kärki, T.; Varis, J. Review of natural fiber-reinforced engineering plastic composites, their applications in the transportation sector and processing techniques. *J. Thermoplast. Compos. Mater.* **2022**, *35*, 1169–1209. [CrossRef]
15. Sanjay, M.R.; Madhu, P.; Jawaid, M.; Senthamaraikannan, P.; Senthil, S.; Pradeep, S. Characterization and properties of natural fiber polymer composites: A comprehensive review. *J. Clean. Prod.* **2018**, *172*, 566–581. [CrossRef]
16. Sun, S.; Li, X. Physicochemical Properties and Fatty Acid Profile of Phoenix Tree Seed and its Oil. *J. Am. Oil. Chem. Soc.* **2016**, *93*, 1111–1114. [CrossRef]
17. Gan, S.-R.; Guo, J.-C.; Zhang, Y.-X.; Wang, X.-F.; Huang, L.-J. "Phoenix in Flight": A unique fruit morphology ensures wind dispersal of seeds of the phoenix tree (*Firmiana simplex* (L.) W. Wight). *BMC Plant Biol.* **2022**, *22*, 113. [CrossRef]
18. Kerni, L.; Singh, S.; Patnaik, A.; Kumar, N. A review on natural fiber reinforced composites. *Mater. Today Proc.* **2020**, *28*, 1616–1621. [CrossRef]
19. Huda, M.K.; Widiastuti, I. Natural fiber reinforced polymer in automotive application: A systematic literature review. *J. Phys. Conf. Ser.* **2021**, *1808*, 012015. [CrossRef]
20. Abdollahiparsa, H.; Shahmirzaloo, A.; Teuffel, P.; Blok, R. A review of recent developments in structural applications of natural fiber-Reinforced composites (NFRCs). *Compos. Adv. Mater.* **2023**, *32*, 26349833221147540. [CrossRef]
21. Choudhary, S.; Haloi, J.; Sain, M.K.; Saraswat, P. Advantages and Applications of Natural Fiber Reinforced Hybrid Polymer Composites in Automobiles: A Literature Review. In *Advances in Modelling and Optimization of Manufacturing and Industrial Systems. Lecture Notes in Mechanical Engineering*; Singh, R.P., Tyagi, M., Walia, R.S., Davim, J.P., Eds.; Springer: Singapore, 2023. [CrossRef]
22. Elfaleh, I.; Abbassi, F.; Habibi, M.; Ahmad, F.; Guedri, M.; Nasri, M.; Garnier, C. A comprehensive review of natural fibers and their composites: An eco-friendly alternative to conventional materials. *Results Eng.* **2023**, *19*, 101271. [CrossRef]
23. Ladaci, N.; Saadia, A.; Belaadi, A.; Boumaaza, M.; Chai, B.X.; Abdullah, M.M.; Al-Khawlani, A.; Ghernaout, D. ANN and RSM Prediction of Water Uptake of Recycled HDPE Biocomposite Reinforced with Treated Palm Waste W. filifera. *J. Nat. Fibers* **2024**, *21*, 2356697. [CrossRef]
24. Saidane, E.H.; Scida, D.; Assarar, M.; Sabhi, H.; Ayad, R. Hybridisation effect on diffusion kinetic and tensile mechanical behaviour of epoxy based flax–glass composites. *Compos. Part A Appl. Sci. Manuf.* **2016**, *87*, 153–160. [CrossRef]
25. Roe, P.J.; Ansell, M.P. Jute-reinforced polyester composites. *J. Mater. Sci.* **1985**, *20*, 4015–4020. [CrossRef]
26. De Albuquerque, A.C.; Joseph, K.; de Carvalho, L.H.; d'Almeida, J.R.M. Effect of wettability and ageing conditions on the physical and mechanical properties of uniaxially oriented jute-roving-reinforced polyester composites. *Compos. Sci. Technol.* **2000**, *60*, 833–844. [CrossRef]
27. Pal, S.K.; Mukhopadhyay, D.; Sanyal, S.K.; Mukherjea, R.N. Studies on process variables for natural fiber composites—Effect of polyesteramide polyol as interfacial agent. *J. Appl. Polym. Sci.* **1988**, *35*, 973–985. [CrossRef]
28. Owolabi, O.; Czvikovszky, T.; Kovacs, I. Coconut-fiber-reinforced thermosetting plastics. *J. Appl. Polym. Sci.* **1985**, *30*, 1827–1836. [CrossRef]
29. White, N.M.; Ansell, M.P. Straw-reinforced polyester composites. *J. Mater. Sci.* **1983**, *18*, 1549–1556. [CrossRef]
30. Sohn, J.S.; Cha, S.W. Enhanced interfacial adhesion of polypropylene and waste wood from roadside trees composite materials. *Int. J. Precis. Eng. Manuf.* **2015**, *16*, 2389–2393. [CrossRef]
31. Pirayesh, H.; Moradpour, P.; Sepahvand, S. Particleboard from wood particles and sycamore leaves. *Eng. Agric. Environ. Food* **2015**, *8*, 38–43. [CrossRef]
32. Aghakhani, M.; Enayati, S.H.; Nadalizadeh, H.; Pirayesh, H. The potential for using the sycamore (*Platus orientalis*) leaves in manufacturing particleboard. *Int. J. Environ. Sci. Technol.* **2014**, *11*, 417–422. [CrossRef]

33. Cu Lao Cham Field Corn Hammock Weaving is a National Heritage. Available online: https://www.vietnam.vn/en/nghe-dan-vong-ngo-dong-cu-lao-cham-la-di-san-quoc-gia/ (accessed on 20 June 2024).
34. *ISO 527-5*; Plastics—Determination of Tensile Properties—Part 5: Test Conditions for Unidirectional Fibre-Reinforced Plastic Composites. International Organization for Standardization: Geneva, Switzerland, 2009.
35. *ISO 527-2*; Plastics—Determination of Tensile Properties—Part 2: Test Conditions for Moulding and Extrusion Plastics. International Organization for Standardization: Geneva, Switzerland, 2012.
36. *Aramis—User Manual Software*; Version 6.1; GOM mbH: Braunschweig, Germany, 2009.
37. Jerabek, M.; Major, Z.; Lang, R.W. Strain determination of polymeric materials using digital image correlation. *Polym. Test.* **2010**, *29*, 407–416. [CrossRef]
38. Quanjin, M.; Rejab, M.R.M.; Halim, Q.; Merzuki, M.N.M.; Darus, M.A.H. Experimental investigation of the tensile test using digital image correlation (DIC) method. *Mater. Today Proc.* **2020**, *27*, 757–763. [CrossRef]
39. Schneider, C.A.; Rasband, W.S.; Eliceiri, K.W. NIH Image to ImageJ: 25 years of image analysis. *Nat. Methods* **2012**, *9*, 671–675. [CrossRef]
40. Abida, M.; Baklouti, A.; Gehring, F.; Vivet, A.; Bouvet, C. Inverse approach for flax yarns mechanical properties identification from statistical mechanical characterization of the fabric. *Mech. Mater.* **2020**, *151*, 103638. [CrossRef]
41. Singh, D.K.; Vaidya, A.; Thomas, V.; Theodore, M.; Kore, S.; Vaidya, U. Finite Element Modeling of the Fiber-Matrix Interface in Polymer Composites. *J. Compos. Sci.* **2020**, *4*, 58. [CrossRef]
42. Inglis, H.M.; Geubelle, P.H.; Matouš, K.; Tan, H.; Huang, Y. Cohesive modeling of dewetting in particulate composites: Micromechanics vs. multiscale finite element analysis. *Mech. Mater.* **2007**, *39*, 580–595. [CrossRef]
43. *Simulia*; Abaqus Documentations; Dassault Systemes: Vélizy-Villacoublay, France, 2019.
44. Baldi, A.; Santucci, P.M.; Bertolino, F. Experimental assessment of noise robustness of the forward-additive, symmetric-additive and the inverse-compositional Gauss-Newton algorithm in digital image correlation. *Opt. Lasers Eng.* **2022**, *154*, 107012. [CrossRef]
45. Baldi, A.; Santucci, P.M.; Bertolino, F. Experimental image dataset for validation of the noise-induced bias that affects Digital Image Correlation. *Data Brief* **2022**, *42*, 108156. [CrossRef]
46. Amraish, N.; Reisinger, A.; Pahr, D.H. Robust Filtering Options for Higher-Order Strain Fields Generated by Digital Image Correlation. *Appl. Mech.* **2020**, *1*, 174–192. [CrossRef]
47. Amraish, N.; Reisinger, A.; Pahr, D. A novel specimen shape for measurement of linear strain fields by means of digital image correlation. *Sci. Rep.* **2021**, *11*, 17515. [CrossRef]
48. Haghdan, S.; Smith, G.D. Natural fiber reinforced polyester composites: A literature review. *J. Reinf. Plast. Compos.* **2015**, *34*, 1179–1190. [CrossRef]
49. Muthukumar, V.; Venkatasamy, R.; Mariselvam, V.; Sureshbabu, A.; Senthilkumar, N.; Fernando, A.A.G. Comparative Investigation on Mechanical Properties of Natural Fiber Reinforced Polyester Composites. *Appl. Mech. Mater.* **2014**, *592–594*, 92–96. [CrossRef]
50. Reddy, S.S.K.; Hussain, S.A. Development and testing of natural fiber reinforced composites with polyester resin. *Int. J. Eng. Sci. Res. Technol.* **2013**, *2*, 2701–2706.
51. El-Wazery, M.S.; El-Elamy, M.I.; Zoalfakar, S.H. Mechanical properties of glass fiber reinforced polyester composites. *Int. J. Appl. Sci. Eng.* **2017**, *14*, 121–131. [CrossRef]
52. Chang, B.P.; Mohanty, A.K.; Misra, M. Studies on durability of sustainable biobased composites: A review. *RSC Adv.* **2020**, *10*, 17955–17999. [CrossRef]
53. Dhir, D.K.; Rashidi, A.; Bogyo, G.; Ryde, R.; Pakpour, S.; Milani, A.S. Environmental Durability Enhancement of Natural Fibres Using Plastination: A Feasibility Investigation on Bamboo. *Molecules* **2020**, *25*, 474. [CrossRef]
54. Sinha, E.; Panigrahi, S. Effect of plasma treatment on structure, wettability of jute fiber and flexural strength of its composite. *J. Compos. Mater.* **2009**, *43*, 1791–1802. [CrossRef]
55. Huber, T.; Biedermann, U.; Müssig, J. Enhancing the fibre matrix adhesion of natural fibre reinforced polypropylene by electron radiation analyzed with the single fibre fragmentation test. *Compos. Interfaces* **2010**, *17*, 371–381. [CrossRef]
56. Pickering, K.L.; Efendy, M.G.A.; Le, T.M. A review of recent developments in natural fibre composites and their mechanical performance. *Compos. Part A Appl. Sci. Manuf.* **2016**, *83*, 98–112. [CrossRef]
57. Faruk, O.; Bledzki, A.K.; Fink, H.P.; Sain, M. Progress report on natural fiber reinforced composites. *Macromol. Mater. Eng.* **2014**, *299*, 9–26. [CrossRef]
58. Beckermann, G.W.; Pickering, K.L. Engineering and evaluation of hemp fibre reinforced polypropylene composites: Fibre treatment and matrix modification. *Compos. Part A Appl. Sci. Manuf.* **2008**, *39*, 979–988. [CrossRef]
59. Baley, C.; Gomina, M.; Breard, J.; Bourmaud, A.; Davies, P. Variability of mechanical properties of flax fibres for composite reinforcement. A review. *Ind. Crops Prod.* **2020**, *145*, 111984. [CrossRef]
60. Peyrache, T.; Chabbert, B.; Aguié-Béghin, V.; Delattre, F.; Kurek, B.; Gainvors-Claisse, A. Multiscale assessment of the heterogeneity of scutched flax fibers. *Ind. Crops Prod.* **2024**, *220*, 119260. [CrossRef]
61. Rajeshkumar, G.; Hariharan, V.; Sathishkumar, T. Characterization of Phoenix sp. natural fiber as potential reinforcement of polymer composites. *J. Ind. Text.* **2016**, *46*, 667–683. [CrossRef]
62. Fiore, V.; Scalici, T.; Valenza, A. Characterization of a new natural fiber from *Arundo donax* L. as potential reinforcement of polymer composites. *Carbohydr. Polym.* **2014**, *106*, 77–83. [CrossRef]

63. Belouadah, Z.; Ati, A.; Rokbi, M. Characterization of new natural cellulosic fiber from *Lygeum spartum* L. *Carbohydr. Polym.* **2015**, *134*, 429–437. [CrossRef]
64. Belaadi, A.; Bourchak, M.; Aouici, H. Mechanical properties of vegetal yarn: Statistical approach. *Compos. B Eng.* **2016**, *106*, 139–153. [CrossRef]
65. de Andrade Silva, F.; Chawla, N.; de Toledo Filho, R.D. Tensile behavior of high performance natural (sisal) fibers. *Compos. Sci. Technol.* **2008**, *68*, 3438–3443. [CrossRef]
66. Kim, J.T.; Netravali, A.N. Development of aligned-hemp yarn-reinforced green composites with soy protein resin: Effect of pH on mechanical and interfacial properties. *Compos. Sci. Technol.* **2011**, *71*, 541–547. [CrossRef]
67. Blanchard, J.M.F.A.; Sobey, A.J.; Blake, J.I.R. Multi-scale investigation into the mechanical behaviour of flax in yarn, cloth and laminate form. *Compos. Part B Eng.* **2016**, *84*, 228–235. [CrossRef]